Hyperacoustic properties and percolation effects in polymer-like lecithin reverse micelles

ARTICLE *in* THE JOURNAL OF PHYSICAL CHEMISTRY · JUNE 1993

Impact Factor: 2.78 · DOI: 10.1021/j100126a034

6 AUTHORS, INCLUDING:

Francesco Aliotta
Italian National Research Council
116 PUBLICATIONS **1,030** CITATIONS
SEE PROFILE

Gaetano Squadrito
Italian National Research Council
44 PUBLICATIONS **1,027** CITATIONS
SEE PROFILE

quite difficult. It has been shown that the width of the filter window is inversely proportional to the degrees of freedom allowable in the subsequent χ^2 minimization routine. Practically, then, one must perform the minimization on the unfiltered spectrum leading to the undesirable consequence of minimization in many parameters of a maximum likelihood estimator that is large and, hence, relatively insensitive to the small changes in parameters that would differentiate between models.

Conclusions

The surface EXAFS of underpotentially deposited silver on gold (111) films on mica was studied with the electrode under potential control. It was revealed that both gold and oxygen are present as backscatterers in the first coordination shell of silver. It was estimated that the bond lengths to gold and oxygen were 2.75 ± 0.05 and 2.42 ± 0.05 Å, respectively, and the respective coordination numbers were 3 and 1. A model consistent with these findings is one where the silver atoms sit on 3-fold sites on the gold surface and have oxygen from water or electrolyte bound at a well-defined distance. This model is qualitatively the same as that proposed for the Cu UPD layer on gold (111) electrodes.

Acknowledgment. This work was supported by the Office of Naval Research, the Materials Science Center at Cornell University, the National Science Foundation, and the Army Research Office. H.D.A. is a recipient of a Presidential Young Investigator Award and an Alfred P. Sloan Fellowship.

Registry No. Ag, 7440-22-4; Au, 7440-57-5.

Aggregation States of Water in Reversed AOT Micelles: Raman Evidence

A. D'Aprano, A. Lizzio, V. Turco Liveri,

Istituto di Chimica Fisica, Universita' di Palermo, Via Archirafi 26, 90123 Palermo, Italy

F. Aliotta,* C. Vasi,

Istituto di Tecniche Spettroscopiche del C.N.R., Via dei Verdi, 98100 Messina, Italy

and P. Migliardo

Istituto di Fisica dell'Universita' and G.N.S.M.-C.I.S.M., Via dei Verdi, 98100 Messina, Italy

(Received: October 6, 1987; In Final Form: January 25, 1988)

Polarized Raman spectra in the O–H stretching region in the water/sodium bis(2-ethylhexyl) sulfosuccinate (AOT)/*n*-heptane system as a function of the molar ratio $R = [H_2O]/[AOT]$ have been measured at 25 °C. By the isotopic substitution ($D_2O \rightarrow H_2O$) method, the unwanted C–H contributions have been eliminated, and a careful analysis of the O–H stretching band was carried out. The results show that the Raman spectra can be partitioned into two contributions linked to the "bonded" and "bulk" water that represent the two "water domains" within the water pool. The percentage, $\alpha(R)$, of the water tightly bonded to the surfactant sheath was evaluated, and its dependence on R gives information about the filling mechanism of the AOT reversed micelles.

Introduction

The behavior of the water close to ions, interfaces, biological membranes, or biopolymers is markedly different than that of bulk water.[1,2] The study of the water properties in these systems allows to understand the nature of the interactions responsible for important phenomena such as interface curvature, ionic solvation, protein folding, and micellization. In particular, the study of the polarization effects on the water entrapped in sodium bis(2-ethylhexyl) sulfosuccinate (AOT) reversed micelles allows to investigate the variation of the local structure of water pools as a function of the size of the reversed micelle core.[3,4]

In relation to the size of the micellar core, different water domains[5] can be identified. For smaller size droplets water exists mainly as bonded H_2O molecules[6,7] whose static and dynamic properties are determined by the local interactions with the negative head groups and the corresponding counterions of the surfactant. As the droplet's size increases, bulk water domains, in dynamic equilibrium with the bonded ones, have been postulated.[8]

The evolution of the droplets size as a function of the molar ratio $R = [H_2O]/[AOT]$ as well as the transport,[9] thermodynamic,[7,10] and spectroscopic[3,4,8,11-14] properties of the water pools has been studied by a large variety of experimental techniques. Even if these studies give a general picture of the micellar core, the different local structures of the water, their relative amounts, and the filling mechanisms[5,10] are still not fully understood.

In order to give more insight into these problems, we present in this paper a Raman scattering investigation on the O–H stretching dynamics of water in the water/AOT/*n*-heptane system. We will show that at any R value the spectrum of the O–H region can be rationalized in terms of the two different contributions associated with bonded and bulk water. The relative amount of

(1) Clifford, J. In *Water: a Comprehensive Treatise*; Franks, F., Ed.; Plenum: New York, 1975; Vol. V, p 75.
(2) Luisi, P. L.; Magid, L. J. *CRC Crit. Rev. Biochem.* **1986**, *20*, 409, and references therein.
(3) Kotlarchyk, M.; Chen, S. H.; Huang, J. S.; Kim, M. W. *Phys. Rev. Lett.* **1984**, *53*, 941.
(4) Kotlarchyk, M.; Chen, S. H.; Huang, J. S.; Kim, M. W. *Phys. Rev. A* **1984**, *29*, 2054.
(5) Nicholson, J. D.; Clarke, J. H. R. In *Surfactant in Solutions*; Mittal, K., Lindman, B., Eds.; Plenum: New York, 1984; Vol. 3, p 1671.
(6) Zinsli, P. J. *J. Phys. Chem.* **1979**, *83*, 3223.
(7) Boned, C.; Peyrelasse, J.; Moha-Onchange, N. *J. Phys. Chem.* **1986**, *90*, 634.
(8) Maitra, A. *J. Phys. Chem.* **1984**, *88*, 5122.
(9) Dreher, K. D.; Hogarty, W. B.; Sydansk, R. D. *J. Colloid Interface Sci.* **1978**, *57*, 379.
(10) D'Aprano, A.; Lizzio, A.; Turco Liveri, V. *J. Phys.* **1988**, *92*, 1985.
(11) Fletcher, P. D. I.; Robinson, B. H.; Tabony, J. *J. Chem. Soc., Faraday Trans. 1* **1986**, *82*, 2311.
(12) Clarcke, J. H. R.; Nicholson, J. D.; Regan, K. N. *J. Chem. Soc., Faraday Trans. 2* **1985**, *81*, 1173.
(13) Mallamace, F.; Migliardo, P.; Vasi, C.; Wanderlingh, F. *Phys. Chem. Liq.* **1981**, *11*, 47, and references therein.
(14) Thompson, K. F.; Gierasch, L. M. *J. Am. Chem. Soc.* **1984**, *106*, 3648.

0022-3654/88/2092-4436$01.50/0

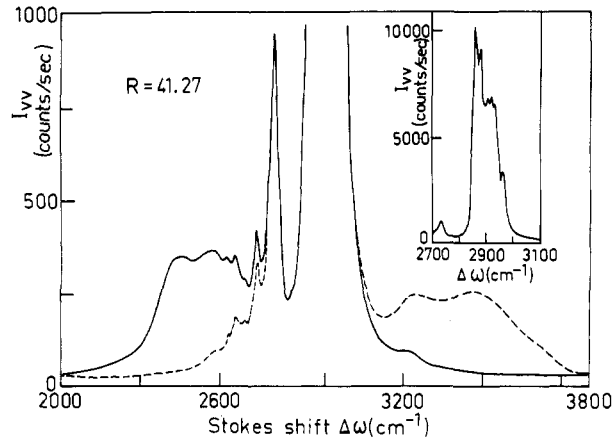

Figure 1. Polarized Raman spectra with light (dashed line) and heavy (full line) water at a molar fraction $R = 41.27$. In the inset the C–H band between 2700 and 3100 cm^{-1} is shown.

the above contributions as a function of R is discussed in light of the existing models.

Experimental Procedures and Results

Sodium bis(2-ethylhexyl) sulfosuccinate (AOT) (Sigma) was purified by using the method described in literature.[15] The purified product was dried under vacuum for several days. The water content (less than 0.4 wt %) of the final product as determined by Karl Fischer titrations was taken into account for the calculation of the R ratio.

n-Heptane (Sigma) was stored on molecular sieves and used without further purification.

Water was deionized and bidistilled laboratory supply. D_2O (Erba RPE, 99.9998%) was used. All the solutions were made up by weight.

Raman spectra were taken with a fully computerized SPEX triple monochromator working at 5 cm^{-1} of band-pass, following a well-established experimental procedure.[16,17] We used a 90° scattering geometry with the 4880-Å line of a Ar^+ Spectra Physics laser as exciting source working at a mean power of ~0.4 W. The measurements were performed, at 25 °C constant temperature, in pure water and in the molar concentration ratio of water to surfactant of 2.41, 10.49, 20.87, 30.78, 41.27, and 58.56, with 0.296 m being the concentration of AOT in *n*-heptane. The Raman spectra were taken in the region 2000–3800 cm^{-1} of the Stokes shift and automatically normalized for the incident beam intensity.

Typical I_{vv} spectra of the AOT reversed micelle ($R = 41.27$) with light water (dashed line) and heavy water (continuous line) are shown in Figure 1. In order to compare the relative intensities of O–D, O–H, and C–H spectral distributions, the intense C–H stretching bands are also shown in the inset of Figure 1.

Assuming that the C–H stretching band changes only in intensity and not in shape either under isotopic substitution or when the water concentration changes, the unwanted C–H contribution can be eliminated by subtracting the deuteriated spectrum from the protonated one. Since these conditions hold, within the experimental uncertainty, for all the systems examined, the integrated C–H area was used as an internal standard to normalize, at each R value, the spectra in D_2O and H_2O. In such a way any experimental errors, such as repositioning of the sample holder, variation in the scattering geometry, and so on, were eliminated.

The polarized O–H stretching band at $R = 41.27$, obtained according to the above procedure, is shown, as an example, in Figure 2. It must be pointed out that such a procedure is necessary since the wings of the C–H band strongly affect the O–H band. As a matter of fact, the C–H shoulder centered at ~3200 cm^{-1} of the Stokes shift modifies the intensity and the shape of the first maximum of the O–H stretching band centered at ~3280 cm^{-1} so that the convolution of the two bands gives rise to a contribution centered at ~3250 cm^{-1}, which was claimed by some authors[18] as connected to a special type of water in the micellar core. It is to be noticed that a similar procedure was successfully applied in the quantitative analysis of the O–H fundamental vibrations in microemulsions[13] and in macromolecular aqueous solutions.[19]

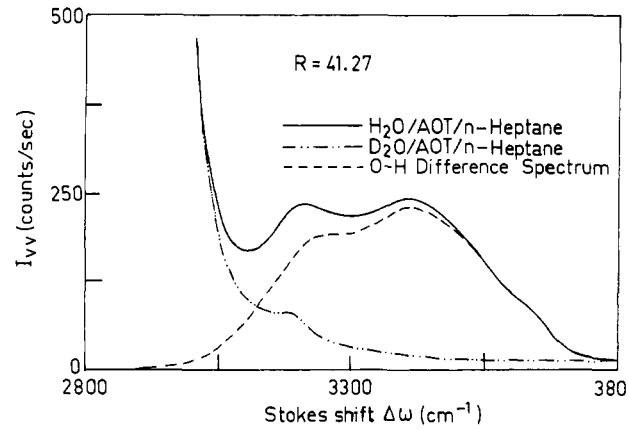

Figure 2. Polarized Raman spectra of the reversed micelles in H_2O and in D_2O at $R = 41.27$, in the 2800–3800-cm^{-1} region. The dashed line is the resulting O–H band after the subtraction of the C–H contribution.

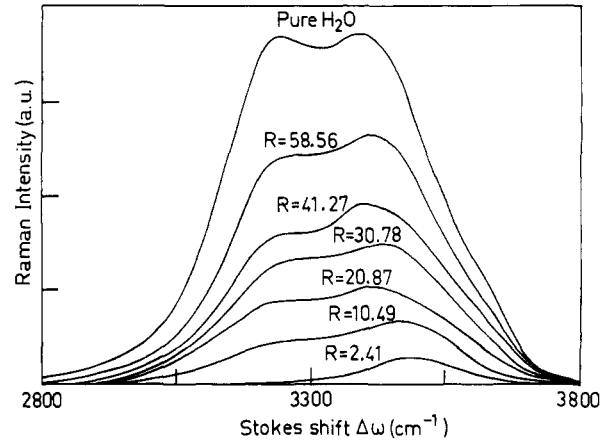

Figure 3. Normalized O–H stretching bands of water in the AOT/*n*-heptane system as a function of R = [water]/[AOT]. Note that the pure H_2O intensity is scaled by a factor of 5.

In order to account for the effective number of scatterers in the scattering volume, the normalized spectra were further corrected for the H_2O concentration.

Figure 3 represents the O–H Raman spectra (evaluated following the above data reduction) at various R and in pure water.

Discussion and Conclusions

The quantitative treatment of the experimental results requires some "a priori" hypothesis on the origin of the vibrational dynamics of the system under analysis. As is well-known, the water internal vibrational dynamics reflect the highly associative nature of the liquid, originated by H-bond-imposed binding effects.[16,17] In a first-order approximation, within a microsphere of radius r (that represents our system), the water can exist in a hydrated sheath of depth d (bonded water) as well as in "bulk water" with different dynamic and static properties. The overall Raman spectrum in the O–H region must therefore reflect the two different dynamic responses.

(15) Politi, M. J.; Brandt, O.; Fendler, J. H. *J. Phys. Chem.* **1985**, *89*, 2345.
(16) D'Arrigo, G.; Maisano, G.; Mallamace, F.; Migliardo, P.; Wanderlingh, F. *J. Chem. Phys.* **1981**, *75*, 4264.
(17) Aliotta, F.; Vasi, C.; Maisano, G.; Majolino, D.; Mallamace, F.; Migliardo, P. *J. Chem. Phys.* **1986**, *84*, 4731.
(18) Biocelli, A. C.; Giomini, M.; Giuliani, A. M. *Appl. Spectrosc.* **1984**, *38*, 537.
(19) Aliotta, F.; Fontana, M. P.; Giordano, R.; Migliardo, P.; Wanderlingh, F. *J. Chem. Phys.* **1981**, *75*, 4307.

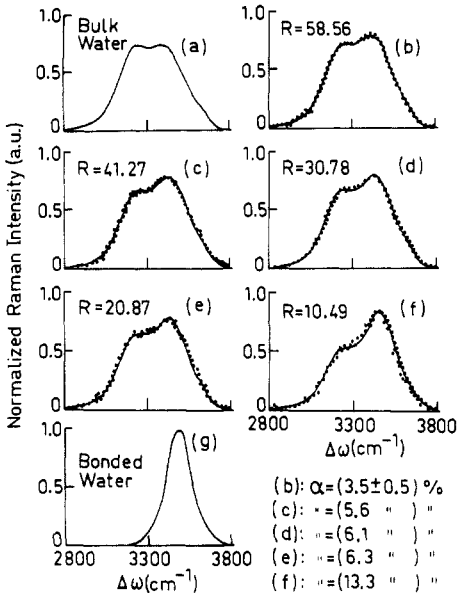

Figure 4. Normalized O–H stretching Raman spectra of water in the AOT/*n*-heptane system as a function of R = [water]/[AOT]. Curves a and g refer to the "bulk" and "bonded" water spectra, respectively. In (b), (c), (e), and (f) the dots are the experimental values and the continuous line represents our fitting by eq 1 (see text). On the bottom the percentage $\alpha(R)$ of the "bonded" water is also reported. Note that spectrum g is scaled by a factor of 1.7.

It must be pointed out that these two types of water are not isotropically distributed into the droplet, but reasonably restricted in two "spatially separated" regions even if the boundary of such regions is not well-defined. The rigid polar head groups and the counterions produce in fact the reorganization of the water molecules in a spatially limited region, with polarization effects slowly decreasing when the distance from the charged ions increases. The fundamental ionic hydration theory and several experimental results[20,21] have evidenced the presence of different hydration shells in aqueous electrolytic solutions with exchange process between the two regions.

Because the exchange processes happen on a time scale longer than the characteristic O–H vibrational times, the Raman probe "sees" as decoupled the various structural local environments.

Under these assumptions we can reasonably assume that the normalized O–H spectrum at any R ratio is due to two different and dynamically separated contributions

$$I_{vv}(\omega) = \alpha(R)I_{vv}^{bonded}(\omega) + [1 - \alpha(R)]I_{vv}^{bulk}(\omega) \qquad (1)$$

where $I_{vv}^{bonded}(\omega)$ and $I_{vv}^{bulk}(\omega)$ are the spectral O–H contributions of the bonded and bulk water, respectively, and $\alpha(R)$ is the fraction of bonded water.

Because the O–H experimental spectrum does not change its shape, within the experimental errors, for $R \leq 2.41$ (as tested by performing measurements at $R = 0.74$ and $R = 0.90$) we assume that the $I_{vv}^{bonded}(\omega)$ spectrum can be represented by the O–H Raman spectrum (curve g of Figure 4) at the molar concentration ratio $R = 2.41$. We have fitted our polarized O–H stretching spectra by eq 1 where the $I_{vv}^{bulk}(\omega)$ spectrum is that of the liquid water at $T = 25$ °C (curve a of Figure 4). The results are shown in Figure 4 where the dots and the full lines of curves b–f are the experimental data and the fitting results, respectively. As can be observed, in spite of the simplicity of the model, the fits are of high accuracy. In the same figure the values of the parameter $\alpha(R)$ are also reported.

Actually, $\alpha(R)$ measures the relative weight of the bonded water spectrum at given R values and coincides with the number of scatterers implied in the bonded structure, normalized to the total number of scatterers, when (i) the partial molar volumes of the bonded and bulk water[10] are evaluated in the fit procedure and (ii) the same scattering efficiency is assumed for both structural environments.

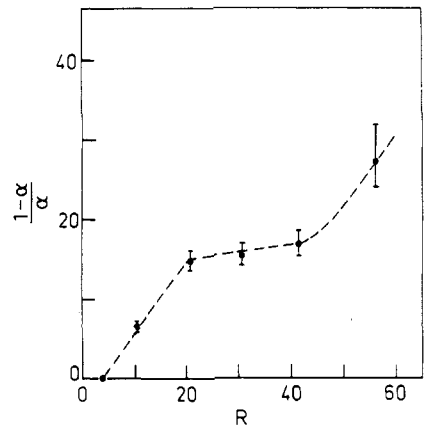

Figure 5. Plot of the ratio between "bulk" and "bonded" water Raman contributions vs R. The dashed line is a guide for the eye.

It is interesting to note that a sizable amount of the dynamical contribution of the bonded water is also implied at the higher molar concentration ratio ($R = 58.56$).

As far as the analysis of the Raman O–H spectrum of the bonded water (curve g of Figure 4) is concerned, we observe that the strong modification occurring in the original water structure at the boundary layer of the microspheres dramatically affects the O–H spectrum of the bulk water (curve a of Figure 4).

It is well-known that the O–H stretching is quite sensitive to the structural modification induced by the solute on the structure of the solvent.[21,22] Obviously, curves a and g of Figure 4 could be deconvoluted in the usual Lorentzian–Gaussian bands, each giving a different degree of polarization of the bond. In such a case the corresponding center frequencies, widths, and areas could be evaluated and assigned to the symmetric and antisymmetric stretchings associated to the local environment. Alternatively, we prefer to assume a structural point of view in order to explain the dynamical properties of the water in different physical environments. Previously,[16] the broadened O–H spectrum of the bulk water was divided into two basic contributions: the first one (centered at 3300 cm^{-1}) was attributed to the tetra-bonded molecules "open water", and the second one (centered at 3450 cm^{-1}) to water molecules having an intermolecular distorted H bond, "closed water". It was also found that the intensity of the first spectral distribution (connected to the icelike form of water) increases as the temperature decreases whereas the intensity of the other band (connected to water implied in distorted bonds) decreases as the temperature decreases.

Comparison of spectra of curves a and g of Figure 4 shows the disappearance of the open water contribution in the bonded water spectrum. This occurrence allows us to support that the primitive highly symmetric structure of the water is destroyed within the sphere of influence of the surfactant. The more compact structure seems to be centered at about the same frequency as the closed water. A similar trend has been observed in the O–H stretching band analysis of aqueous electrolytic solutions such as $CuBr_2$,[21] $ZnBr_2$,[23] and $NaNO_3$,[22] so confirming our starting hypothesis that Raman scattering, as far as intramolecular vibrational modes are concerned, is sensitive only to the first hydration shell around the ions.

In order to quantify the concentration dependence of the two different water structures (seen by Raman probe), the ratio between the number of scatterers associated with the "bulk" water ($1 - \alpha$) and the number of scatterers associated with the water bonded to the surfactant (α) is reported in Figure 5 as a function

(20) Vaslow, F. In *Water and Aqueous Solutions*; Horn, R. A., Ed.; Wiley-Interscience: New York, 1972; p 465.
(21) Aliotta, F.; Maisano, G.; Migliardo, P.; Vasi, C. *Phys. Chem. Liq.* **1982**, *12*, 69.
(22) Rull, F.; De Saja, J. A. *J. Raman Spectrosc.* **1986**, *17*, 167.
(23) Aliotta, F.; Fontana, M. P.; Maisano, G.; Migliardo, P.; Wanderlingh, F. *Opt. Acta* **1980**, *27*, 931.

of R. The slope of the curve, always positive, indicates that as R increases (i.e., the water content increases), the number of H_2O molecules dynamically seen as bulk water increases. In the range $20 < R < 40$ a different slope is observed. This occurrence seems to be indicative of a mechanism (droplets aggregation?) in the growth process of the reversed micelles. On this basis, by following the evolution of the $(1 - \alpha)/\alpha$ ratio against R, the filling mechanism of AOT reversed micelles can be explained in terms of an initial hydration of the head groups of the surfactant followed by the formation of a water pool where a continuous equilibrium between bonded and bulk water can exist.

Conclusively, we can assert that a boundary layer of water (bonded water), with a structure different from that of bulk water, is evidenced through the Raman scattering experiment. At any value of R, the O–H stretching contribution is interpreted as originating from two coexisting spatially separated structural arrangements for the water: the first one is surfactant imposed, and the second one is the usual water structure. The relative amount of the bonded water is estimated as a function of the molar ratio R.

Registry No. AOT, 577-11-7; H_2O, 7732-18-5.

Catalytic and ESR Studies of Ethylene Dimerization on Palladium-Exchanged Na–X and Ca–X Zeolites

Ashim K. Ghosh and Larry Kevan*

Department of Chemistry, University of Houston, Houston, Texas 77004 *(Received: October 15, 1987)*

Oxygen-pretreated, palladium-exchanged Na–X and Ca–X zeolites are catalytically active for ethylene dimerization in both static and flow reactors. The catalytic activity of the zeolites for this reaction is shown to be due to palladium species and is greatly dependent on the type of major cocation (Na^+ or Ca^{2+}) in the zeolites. The cocations influence the location of the active palladium species. In NaPd–X zeolites, palladium cations occupy sites (SI or SI′) which are inaccessible to ethylene, while in CaPd–X zeolites palladium cations occupy sites (SII′ or SII) which are relatively accessible to ethylene. As a result, the reaction occurs after a longer induction period in NaPd–X zeolites due to migration of palladium species toward more accessible locations. This induction period decreases with an increase of reaction temperature. Paramagnetic species, giving ESR signals at $g_\parallel = 2.53$ and $g_\parallel = 2.33$–2.34, both with $g_\perp$ at 2.10, are assigned to Pd^+ coordinated to ethylene and are detected prior to butene formation. Consequently, monovalent palladium cations are considered to be catalytically active sites for ethylene dimerization.

Introduction

Several papers[1-4] have treated ethylene dimerization on Pd-exchanged zeolites. It is generally accepted that palladium species directly participate in the formation of catalytically active sites. However, the oxidation and coordination states of the palladium species are uncertain. It has been speculated that monovalent[2] or divalent[4] palladium cations are catalytically active in promoting ethylene dimerization.

The catalytic efficiency of a cation-exchanged zeolite for nonacid catalysis is dependent on the type, amount, and location of active cations in the zeolite structure.[5-8] Recent work[9] in this laboratory has shown that transition-metal-cation location in a zeolite can be controlled by a number of factors including (a) the charge and size of the more abundant cocation, (b) the Si/Al ratio, (c) the structural type of zeolite, (d) the thermal pretreatment, and (e) the presence of various adsorbates. Of these factors the use of cocation variation as a control method seems particularly promising.

In preliminary work,[4] it was shown that, irrespective of palladium concentration, CaPd–X zeolites are active for ethylene dimerization. In contrast, only higher palladium loadings in PdNa–X zeolite were shown to be active. This was explained by the different locations of the active palladium cations dependent on the presence of Na^+ versus Ca^{2+} cocations. In NaPd–X the Pd cations occupy relatively inaccessible sites, while in CaPd–X the Pd cations occupy more accessible sites with respect to ethylene.

The present work describes studies of ethylene dimerization on palladium-exchanged Na–X and Ca–X zeolites using both static and flow reactors. Using electron spin resonance (ESR) spectroscopy, the generation and migration of paramagnetic palladium species are monitored before and during the reaction. By comparison of catalytic and ESR results the formation and location of catalytically active palladium sites are assessed. The effect of using static versus flow reactors is also compared.

Experimental Section

Linde Na–X zeolite was obtained from Alpha Chemicals. Ca–X zeolite was prepared from Na–X by ion exchange with 0.1 M $CaCl_2$ solution at 80 °C for 1 week. Palladium was introduced into the zeolite as $Pd(NH_3)_4^{2+}$ cation by ion exchange with various amounts of 0.01 M palladium tetraammine chloride (Alpha) solution at room temperature for 24 h. Commercial atomic absorption was used to determine the palladium content. Most experiments were done with samples of $CaPd_{1.7}$–X, $CaPd_{9.6}$–X, and $NaPd_{12.5}$–X zeolites where the subscript refers to the number of palladium ions per unit cell. Some experiments were done with Ca–X and $NaPd_{1.6}$–X zeolites. Premixed ethylene (4 wt %) in He, ethylene, 1-butene, *cis*-2-butene, and *trans*-2-butene were obtained from the Linde Division of Union Carbide Corporation.

Experiments were carried out by using a fixed bed type reactor made of glass with either continuous gas flow at atmosphere pressure or a closed, static reactor system of total internal volume

(1) Lapidus, A. L.; Mal'tsev, V. V.; Garanin, V. I.; Minachev, Kh. M.; Eidus, Ya. T *Izv. Akad. Nauk SSSR, Ser. Khim.* **1975**, 2819.
(2) Lapidus, A. L.; Mal'tsev, V. V.; Shpiro, E. S.; Antoshin, G. V.; Garanin, G. V.; Minachev, Kh. M. *Izv. Akad. Nauk SSSR, Ser. Khim.* **1977**, 2454.
(3) U.S. Patent 3 738 977, 1973.
(4) Michalik, J.; Lee, H.; Kevan, L. *J. Phys. Chem.* **1985**, *89*, 4282.
(5) Maxwell, I. E. *Adv. Catal.* **1982**, *31*, 1.
(6) Lunsford, J. H. *Catal. Rev.* **1975**, *12*, 137.
(7) Ben Taarit, Y.; Che, M. In *Catalysis by Zeolites*; Imelik, B., et al., Eds.; Elsevier: Amsterdam, 1980; p 67.
(8) Smith, J. V. In *Zeolite Chemistry and Catalysis*; Rabo, J. A., Ed.; American Chemical Society: Washington, D.C., 1976; Chapter 1.
(9) Kevan, L. *Acc. Chem. Res.*, **1987**, *20*, 1.

0022-3654/88/2092-4439$01.50/0